Journal of Materials Chemistry A

ROYAL SOCIETY OF CHEMISTRY

PAPER

View Article Online
View Journal | View Issue

Cite this: J. Mater. Chem. A, 2024, 12, 1746

An energy harvester based on UV-polymerized short-alkyl-chain-modified [DBU][TFSI] ionic liquid electrets†

Topias Järvinen, ‡*[a] Nemanja Vucetic,‡[b] Petra Palvölgyi,‡[a] Olli Pitkänen, [a] Tuomo Siponkoski, [a] Helene Cabaud,[b] Robert Vajtai, [c] Jyri-Pekka Mikkola[bd] and Krisztian Kordas[a]

Three short-alkyl-chain-modified [DBU][TFSI] ionic liquids (ILs) were synthesized and utilized in electrets. The electrets were prepared by mixing a UV-curable polymer with the ionic liquids followed by polymerization while applying an external electric field, thus forming spatially separated anions and cations in the proximity of opposing surfaces of the composite slabs. The immobilized surplus surface charge was measured by periodically engaging the electret with a metal counter electrode plate and detecting the displacement current using a charge amplifier. The results show that electrets based on polymerized [DBU][TFSI] ILs have a separated surface charge density of up to 64 nC × cm^{-2}, which equals an energy harvesting density of 7.0 nJ × cm^{-2}. Control measurements repeated after a few days to assess the stability and reproducibility of the systems showed that while charge separation reverses over time to some extent, the polymerized ionic liquid samples are resilient to exposure to atmospheric conditions and could be utilized in this type of energy harvesting scheme.

Received 7th September 2023
Accepted 10th December 2023

DOI: 10.1039/d3ta05448a

rsc.li/materials-a

Introduction

In light of the global efforts towards de-carbonizing our society and industry, technologies associated with alternative green energy sources, generators (converters) and storage devices have become even more important and relevant than before. General concepts with efficient mechanical-to-electrical power conversion are now clearing their way toward autonomous power management of low-power energy harvesters (up to a few mW), including environmental and health sensors as well as wireless devices such as Bluetooth and RFID tags. New integrated energy scavenging devices not only offer environmentally friendly and self-sustainable power sources but can also reduce the role of disposable batteries in backup power supplies. The multimode and low-frequency characteristics of human biomechanical movement make efficient energy harvesting a challenging task, particularly when the comfort of the user needs to be addressed. The most common portable kinetic energy harvesting devices are based on piezoelectric, electromagnetic, triboelectric, and electrostatic mechanisms. The electrostatic harvesters are, however, usually vibration-based thus having optimal resonant frequencies up to several magnitudes higher than human motion (>100 Hz).[1] Therefore, triboelectric, piezoelectric, and electromagnetic energy harvesters have been the most commonly reported techniques for human motion.[2] In electromagnetic and piezoelectric portable energy harvesters, the typical reported power densities have been in the range of a few tens of mW cm^{-2}.[3–7] Triboelectric energy harvesters, on the other hand, have been reported to provide power densities one order of magnitude higher,[8] but the values are often derived from the peak/instantaneous power in contrast to the average power. Also, high impedance and high generated voltages make electrical coupling cumbersome, while some recent results show that advanced switch-based harvesting circuitry is beneficial to be utilized also with triboelectrics.[9] Due to the high variety of available flexible and soft cost-effective materials, the triboelectric energy harvesting technique has become the most common approach to collecting biomechanical energy for portable devices.[2]

A newly emerging harvesting concept is based on electrostatic energy conversion utilizing polarized and polymerized soft electrets, which can provide comfortable/unobtrusive energy harvesting schemes for wearable soft electronics.[10] A great benefit of the operating principle is its reduced

[a]Microelectronics Research Unit, Faculty of Information Technology and Electrical Engineering, University of Oulu, FI-90014 Oulu, Finland. E-mail: topias.jarvinen@oulu.fi

[b]Laboratory of Industrial Chemistry and Reaction Engineering, Johan Gadolin Process Chemistry Centre, Åbo Akademi University, Henriksgatan 2, Turku/Åbo 20500, Finland

[c]Department of Material Science and NanoEngineering, Rice University, Houston, Texas 77005, USA

[d]Technical Chemistry, Department of Chemistry, Chemical-Biological Center, Umeå University, SE-90187 Umeå, Sweden

† Electronic supplementary information (ESI) available. See DOI: https://doi.org/10.1039/d3ta05448a

‡ These authors contributed equally to the manuscript.

dependency on inertial forces (in contrast to piezoelectric charge generators) and thus energy harvesting may be carried out in a broad vibration frequency spectrum (in contrast to piezoelectric harvesters, which usually show efficient generation in resonance mode only). In the newest generation of electrostatic harvesters, recently, a very elegant structure was proposed for the electrets. Instead of solid-state electret plates, polarized gels of ionic liquids are used so that the anions and cations are separated at the top and bottom of the structure by an electric field before the curing of the gel.[11–13] Upon pressing the flexible gel electrets with conductive surfaces both the contact area and the electrode spacing change, thus inducing current in the external circuit. Induced current densities of ~2 $\mu A\ cm^{-2}$ over a 10 MΩ external load have been successfully measured.[12] In another inspiring concept of a vibrational harvester, the [DEME][TFSA] ionic liquid was used to generate several nW power by squeezing and drawing the electret between a pair of vibrating electrodes.[11] A slightly modified approach was used with ionic liquids dispersed in a polymer matrix. In this hybrid material, the [TMPA][TFSI] ionic liquid was mixed with a photo-curable monomer and initiator and cured by UV exposure. Changes in the contact areas by mechanical compression and drawing of the solidified ionic liquid between a pair of electrodes at 15 Hz resulted in a current output of 22 $\mu A_{p-p}\ cm^{-2}$ at 1.5 V.[13] The energy harvesting electrets have also been referred to as EDLEs (electric double layer electrets), which are also used in contactless energy harvesting.[14,15] Free radical photo-polymerization (UV-curing) is a well-known technique that is performed at room temperature under UV radiation in the presence of an appropriate free radical photo-initiator. This technique has an advantage compared to conventional routes as it allows fine-tuning of the polymer properties while being versatile, fast, and easy to use. It is environmentally friendly as the energy consumption is relatively low and there is no emission of organic compounds since it is performed in a solvent-free environment.[16–20] The low-viscosity 1-ethyl 3-methyl imidazolium dicyanamide [EMIM][DCA] IL in PVdF-HFP provided charge carriers with greater mobility during charge separation. The conductivity of the pure polymers was in the range of $1.2 \times 10^{-6}\ S\ cm^{-1}$ and it increased up to $3.4 \times 10^{-3}\ S\ cm^{-1}$ when 25 wt% IL was incorporated; at higher loadings, the free-standing nature of the sample was lost and the IL leaked from it.

The choice of the ionic liquid plays a crucial role since its characteristics are affected by the structure of both cations and anions.[21] It was found that the choice of the anion has the most important influence on IL properties, and most importantly, on water miscibility which is very relevant for electrochemical applications. Water content is the main factor influencing the electrochemical window (EW) of ionic liquids, narrowing both cathodic and anodic limits, most probably as a consequence of water electrolysis.[22–25] Hydrophobic anions are represented by BF_4, PF_6 and TFSI. Even though BF_4 and PF_6 are reported to show large electrochemical stability, their limited hydrolytic stability and forthcoming release of HF and other species limit their more extensive usage in IL chemistry.[26] Besides this, it was found that for TFSI-based ILs with a similar cation, EWs are wider than those for BF_4-based ILs.[27,28]

Finally, an ideal IL electrolyte should have a wide electrochemical window, low volatility, good thermal stability, low viscosity, and high ionic conductivity. Most common ILs are based on dialkyl imidazolium cations, which possess an electrochemically active hydrogen in the C2 position of the imidazole ring making them not applicable for electrochemical processes.[29] On the other hand, organic superbases such as 1,8-diazabicyclo- [5.4.0]undec-7-ene (DBU) possess highly reactive imine nitrogen in the heterocyclic ring that can build stable cationic structures through the quaternization reaction. Various alkylated superbase-derived ionic liquids with the TFSI anion have already been designed and their main physicochemical properties, including melting points, decomposition temperatures, density, viscosity, and electrochemical properties, were studied extensively.[29–32] It was found that they have ionic conductivities in the range of 3.2–3.5 $mS\ cm^{-1}$ and exhibit good electrochemical stability with EWs ranging from 4.3 to 4.6 V, which is wider than those of the common 1,3-dialkylimidazolium ionic liquids making them a logical choice for electrochemical devices.[29]

In our study, we synthesized short alkyl chain modified [DBU][TFSI] ionic liquids by 1,8-diazabicyclo-[5.4.0]undec-7-ene alkylation with halo-ethane, butane, and hexane, coordinated with the TFSI anion, which was assumed to meet the required characteristics for application in a new type of energy harvesting device. The corresponding ionogel matrices with spatially separated cations and anions were prepared by the photo-polymerization of poly(ethylene glycol) diacrylate (PEGDA) in the presence of an external electric field and tested as electret materials in a new type of oscillating energy harvester. The concept was proven, and the results showed that the generated energy density of the prepared electrets was up to $7.0\ nJ \times cm^{-2}$ which equals 5.5 nJ generated energy per each cycle, making them already suitable candidates to harvest energy from mechanical motion for a diverse range of portable applications, which could be further enhanced with a tuned spring-mass structure.

Results and discussion

In the first part of the study, we explored the influence of the amount of ionic liquid in the polymer matrix on the overall performance of the ionogel to find the optimum compositions (Table S1, in the ESI†). The energy conversion density of ionogels was found to increase linearly as a function of IL concentrations up to 20 wt%, while the electrets were most stable at 10 wt% or lower. On the other hand, an excessive amount of IL can compromise the polymerizability of ionogels and at concentrations exceeding 20 wt%, mechanical deterioration and leaking of samples were observed and, thus the stability and reusability of the materials were compromised. Average Young's modulus for the samples was 23.36 MPa with a standard deviation of 3.21 MPa and did not show correlation to IL concentrations with the exception of the 20 wt% sample (17.82 MPa). However, the yield strengths measured for this

sample and polymer reference without any IL were 5.5 MPa and 17.98 MPa, respectively, which indicates the effect of incorporating ILs into the polymer structure.

Only fully polymerized and stable electrets were selected for charge generation measurements. The reference sample, containing only the polymer and photoinitiator without any ionic liquid, was used for a baseline measurement. In Fig. 1c, representing typical charge integrator outputs plotted using an oscilloscope, some charge generation can be observed even with the reference sample. This is attributed to static and triboelectric effects as well as parasitic capacitances between the electret and the measurement system. In addition to the reference sample, typical charge generation curves are shown for electrets with 1 and 10 wt% ionic liquid contents, respectively, showing clearly enhanced responses. It is worth noting that the response between the anodic and cathodic sides of the electret was not symmetrical, which we attribute to the different charge densities of the separated ions on the surfaces. However, as seen in the statistical analysis, asymmetry is reduced after a few days, along with the deviation within samples. It's also notable that while the initial charge generation at contact point charges of the sample capacitor is fast, the discharging is much slower. This limitation, caused by the amplifier characteristics, limited the oscillation frequency to 0.1 Hz.

The charge generation measurements were repeated after a few days to assess the stability of the polymerized electrets from different ILs as shown in Fig. 2. The first set of measurements, Fig. 2a, was performed right after polymerization. In the case of [DBU-C2][TFSI], the generated charge didn't increase significantly with 15 and 20 wt% compared to 10 wt% IL. Thus, the 10 wt% loading was repeated in the case of [DBU-C4][TFSI] and [DBU-C6][TFSI] ILs. The highest charge generation at 10 wt% IL was achieved with [DBU-C4], while the charge generated by C2 was comparable with that of C6. On the last day of experiments, 10.3 to 25.7% of the original charges for the 10 wt% samples were retained, Table 1. The charge retention for different concentrations of C2 ranged from 16.7 to 9.1% for 1 and 20 wt%, respectively.

The energy E in the known capacitor C charged to voltage V was calculated as

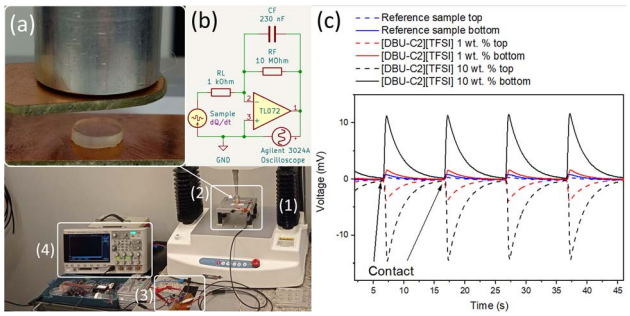

Fig. 1 (a) Charge measurement setup including (1) the texture analyzer, (2) sample and electrodes, (3) charge amplifier circuit and (4) oscilloscope. Inset shows the electret sample and electrodes in detail. (b) A simplified schematic of the charge amplifier circuit. Example waveforms from the charge amplifier circuit output in (c).

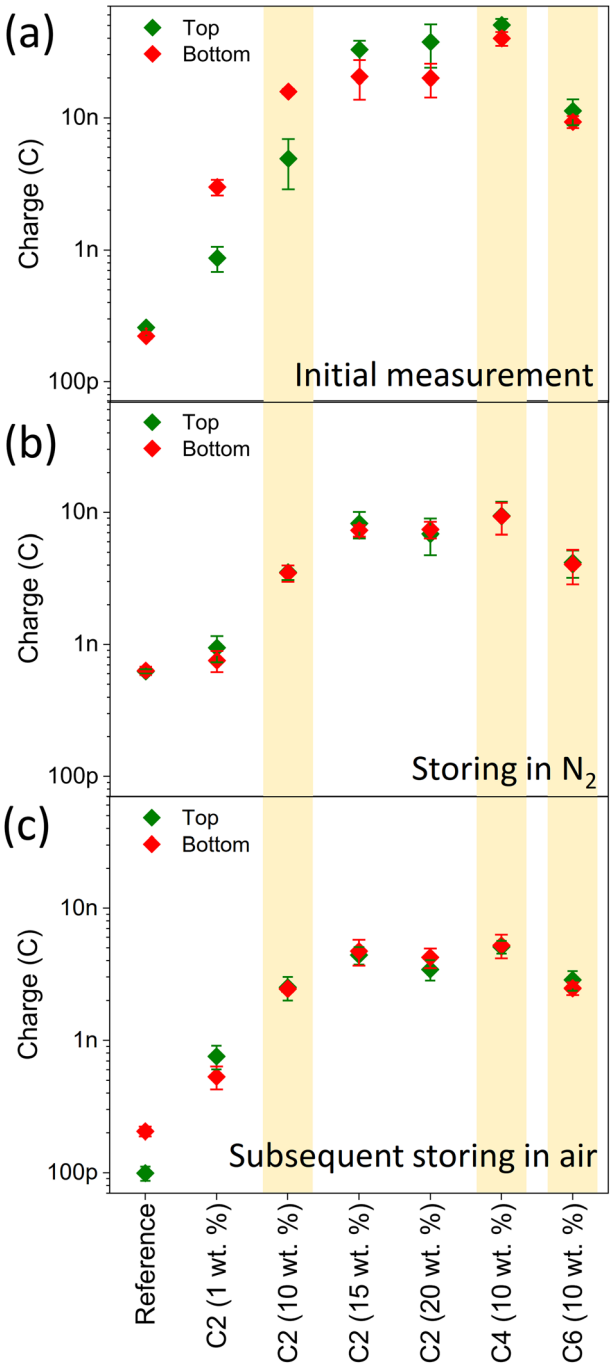

Fig. 2 Charge generation stability of the [DBU-C2/C4/C6][TFSI] samples over time, (a) measured right after polymerization, (b) when stored in N_2 for at least 3 days and (c) after an additional 3 days of exposure to air. Highlighted values are for 10 wt% samples for the different ILs. Top/bottom refers to the orientation of the electret in the ion separation and polymerization process (Fig. 4), where the top side is negatively charged with an excess of anions against the positive electrode and *vice versa* in the case of the bottom electrode.

$$E = 0.5 \times C \times V^2 = 0.5 \times Q \times V \quad (1)$$

In the detachment phase of the cycle, an opposing current is generated when the electret is detached from the electrode. This

Table 1 Performance of the electrets with 10 wt% IL over time

Sample	Mean charge generation on day 0 (nC)	Energy stored in the capacitor (nJ)	Mean charge generation after 3 days of exposure to air (nC)	Charge generation retention (%)
[DBU-C2][TFSI] 10 wt%	15.8 ± 0.8	0.5	2.4 ± 0.1	15.8
[DBU-C4][TFSI] 10 wt%	50.4 ± 5.8	5.5	5.2 ± 1.1	10.3
[DBU-C6][TFSI] 10 wt%	11.3 ± 2.5	0.3	2.9 ± 0.5	25.7

current could be harvested as well with a rectifying circuit, thus doubling the generated energy in one cycle. As the surface area of the electret is 0.79 cm^2, the normalized charge and energy per area were approximately 14–64 nC × cm^{-2} and 0.4–7.0 nJ × cm^{-2}, respectively.

The power output of the charge generator depends on the oscillation frequency. Due to charge amplifier characteristics, a low frequency of 0.1 Hz was used, resulting in 40 to 700 pW × cm^{-2} average output power density. However, in actual energy harvesting applications the oscillation frequency will be considerably higher providing a greater sustained power output. For example, in typical ranges of tens of Hz, the power output is already in a range of tens to hundreds of nW, which is typical of ionic liquid-based energy harvesters.[33–35]

When comparing Fig. 2a and b, it is evident that the performance of the harvester is declining upon storage of the samples. It can be hypothesized that this is evidence of preserved fluidity of ionic liquids and mobility of the ions within the polymer framework. When samples are not in use in the harvester, ions that were initially separated tend to get back together and pair up from the surface back to the bulk. This was also observed by XPS analysis (Fig. S2†) by tracking the atomic concentration of fluorine, as a main element of the anion. Fluorine concentration in the surface of the samples (usually reported XPS penetration depths of 2–5 nm) decreased ~2 at% during 5 days of storage on both sides of all the tested samples with 10 wt% [DBU-C4][TFSI] regardless of the sample polarization. Further investigation would be needed in order to better understand the deactivation mechanism and suppress it in future materials. However, Fig. 2c displays the stability of the samples when exposed to atmospheric conditions and moisture, making them a suitable material for applications under standard room atmosphere conditions. The XPS analysis did not show systematic differences in the elemental concentration between the samples with different polarizations. This is because the excess of separated ions is miniscule compared to the high concentration of both cations and anions in the electret materials.

The densities and molar masses of ionic liquids and polymer (1.12–1.4 g ml^{-1}[29] and 461.44–575 g mol^{-1}, respectively) were approximated to be similar. From these values, the molar concentration of ions in the electret materials could be estimated. The two last columns in Table 2 compare the calculated charge of the ions in the layer volume (visible with XPS) against the measured surplus (*i.e.*, separated) charge in experiments. The ratios between them indicate that less than 1% of the total charges in this layer volume are separated, which could be observed by the integrator circuit in the charge generation experiment.

Experimental

Materials

The monomer poly(ethylene glycol) diacrylate (PEGDA, Mn = 575 g mol^{-1}) and photoinitiator 2-hydroxy-2-methyl-1-phenyl-1-propanone (HMPP) were purchased from Sigma-Aldrich. Ionic liquids were synthesized in-house using 1,7-diazabicyclo[5.4.0] undec-7-ene (DBU) obtained from TCI chemicals that were vacuum dried and stored with molecular sieves before use. Bromoethane, 1-iodobutane, 1-chlorohexane, bis(trifluoromethanesulfonyl)-imide (TFSI) and all the solvents and other chemicals were of analytical grade, purchased from Sigma Aldrich and Alfa Aesar and used as obtained without additional purification.

Synthesis of ionic liquids

The quaternization reaction. Ionic liquids with alkyl moieties were synthesized *via* a modified synthetic procedure adopted from the literature,[32,36] as illustrated in Fig. 3. In the

Table 2 Calculated concentrations, chemical amounts (n_{IL}) of ILs and corresponding charges of anions and cations in a layer volume with a thickness of 5 nm (typical probing depth of XPS) as well as measured surplus charges assessed using the integrator circuit

SAMPLE	Concentration of IL *i.e.* c_{IL} (mol dm^{-3})	Amount of IL *i.e.* n_{IL} in layer volume (mol)	Charge in layer volume (C)	Measured separated charge (C)
[DBU-C2][TFSI] 1%	0.02	9.56×10^{-12}	9.22×10^{-7}	$3.0 \pm 0.4 \times 10^{-9}$
[DBU-C2][TFSI] 10%	0.25	9.77×10^{-11}	9.43×10^{-6}	$1.6 \pm 0.8 \times 10^{-8}$
[DBU-C2][TFSI] 15%	0.38	1.48×10^{-10}	1.43×10^{-5}	$3.3 \pm 0.5 \times 10^{-8}$
[DBU-C2][TFSI] 20%	0.52	2.00×10^{-10}	1.93×10^{-5}	$3.7 \pm 1.3 \times 10^{-8}$
[DBU-C4][TFSI] 10%	0.23	9.21×10^{-11}	8.88×10^{-6}	$5.0 \pm 0.6 \times 10^{-8}$
[DBU-C6][TFSI] 10%	0.22	8.71×10^{-11}	8.40×10^{-6}	$1.1 \pm 0.2 \times 10^{-8}$

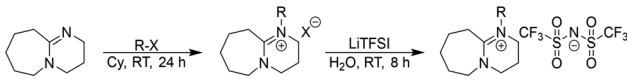

Fig. 3 Ionic liquid synthesis reactions.

first step, the quaternization reaction was performed in a round bottom flask of 250 ml volume containing 100 ml cyclohexane. 0.1 mol of 1,8-diazabicyclo(5.4.0)undec-7-ene (DBU) was placed in the reactor and 0.15 mol of bromoethane, 1-iodobutane or 1-chlorohexane was dropwise added while cooling the reactor in an ice bath. The reactor was sealed, and the reaction slurry was stirred with a magnetic stirrer at room temperature for the next 24 h, during which a solid salt was formed as a separate phase. After the reaction, the supernatant layer of the solvent containing unreacted compounds was precipitated and residual halogen salt was washed with 200 ml of diethyl ether and decanted, followed by vacuum drying at 80 °C for 4 h. The as-obtained material was collected and preserved in a sealed vial under atmospheric conditions until further use.

Anion metathesis. Halide anions were exchanged *via* the anion metathesis reaction.[29,37] In a round bottom flask supplied with a magnetic stirrer, 20 ml of deionized water was loaded and 0.01 mmol of bis(trifluoromethane)sulfonamide lithium salt was dissolved. Next, an equimolar amount of the quaternized DBU salt obtained from the previous step was added to the stirred solution. The reaction mixture was sealed and left to react under vigorous stirring for 8 h at room temperature, forming a separate liquid organic phase. After the reaction, the slurry was transferred into a separatory funnel and the organic phase was extracted with 150 ml of dichloromethane. The thus obtained solvent was dried overnight with an excessive amount of $MgSO_4$ drying agent, followed by filtration. Next, the collected, purified organic phase was transferred to a round bottom flask and the solvent was removed under reduced pressure at 90 °C for 12 h to give an ionic liquid of a high purity. The obtained product was weighed and preserved in a sealed vial with molecular sieves under atmospheric conditions until further use. After obtaining the ionic liquids, they were characterized by various analytical techniques. With elemental analysis (EA), ^{1}H NMR and ^{13}C NMR, it was possible to characterize the structures of the compounds.

Preparation of ionogel electrets

The ionogels were prepared by UV-assisted polymerization of poly(ethylene glycol) diacrylate (PEGDA) and the 2-hydroxy-2-methyl-1-phenyl-1-propanone (HMPP) photoinitiator in the presence of different ILs ([DBU-C2][TFSI], [DBU-C4][TFSI] and [DBU-C6][TFSI]) under an external electric field. First the monomers, photoinitiator (monomers : photoinitiator ratio = 99 : 1) and ionic liquid (with concentrations of 1, 10, 15 and 20 wt% in the mixture) were measured into a glass vessel and mixed for 30 min with a magnetic stirrer. Ionic liquid concentrations above 20 wt% were found to be unstable. The mixture was then poured into a cavity of a polyvinylidene fluoride ring (with a thickness and inner diameter of 2.0 and 10 mm, respectively) placed at the bottom metal electrode and covered with an ITO-coated glass electrode (the polymer ring serves both as a mold for the material and as the spacer for the electrodes). The current through the samples was measured using a multimeter (Fluke 289 True-RMS Multimeter) in the electric circuit. First, 2.5 V DC electric potential was applied between the electrodes resulting in an electric field of 1250 V × m^{-1}, and then after 5 min, polymerization was initiated by UV light (365 nm and 1500 mW) and these conditions were maintained from 7 minutes up to 18 minutes, until the current drop stabilized (Fig. S1†). The preparation of the polarized PEGDA-IL samples was done in air at room temperature. A schematic describing the charge separation and polymerization process is presented in Fig. 4.

Characterization

All the ^{1}H and ^{13}C NMR spectra of the synthesized ILs were characterized in chloroform-d at room temperature (298 K) on an Avance-III HD 500 MHz spectrometer, Bruker Co., equipped with a Bruker SmartProbe™. The content of carbon, hydrogen, nitrogen, and sulfur was analyzed with a CHNS analyzer, FLASH 2000, Thermo Fisher Scientific Inc. The results are reported as average values of five analyses in the ESI.† The water content of ionic liquids was detected by coulometric Karl Fischer (KF) titration with an automatic coulometric titrator Metrohm 851, Titrando instrument connected to an 860 KF Thermoprep oven. The KF measurements were performed under a dry N_2 gas atmosphere of a 90 ml min^{-1} flow rate, at 110 °C. The water content was reported as an average value of three measurements for each sample; in the measurements approximately 100 mg sample mass was sealed in a glass vial tube. X-ray photoelectron spectroscopy (XPS) analysis of the polymerized ionogel electrets was performed using an Escalab 250 XI system with an Al Kα X-ray source, 1486.6 eV, Thermo Fisher Scientific Inc., and the data was evaluated with Avantage software. Further characterization such as thermal stability analysis,

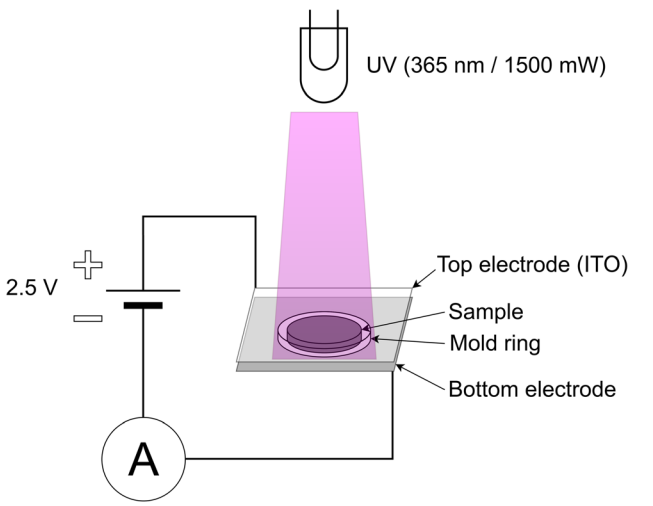

Fig. 4 Experimental setup for charge separation and polymerization of the electret samples.

electrochemical windows (4.7 V for [DBU-C2][TFSI] and [DBU-C4][TFSI] and 4.8 V for [DBU-C6][TFSI]) and conductivities of the ILs was carried out in a separate study where the ILs were assessed as supercapacitor electrolytes.[38]

Charge generation measurements

The charge generated by the polymerized electret samples was measured with a custom test setup (Fig. 1a), which consisted of three elements. The displacement between the sample and electrode was implemented with a texture analyzer (TA.HD-*plus*C, Stable Micro Systems, UK). The contact force between a stationary ionic gel sample and the moving electrode was normalized to 10 N and the electrode was repeatedly brought into contact by oscillating sinusoidally with a 10 mm amplitude and 0.1 Hz frequency. The generated charge in the electrode was fed to a custom charge integrator circuit (Fig. 1b), utilizing an operational amplifier (TL072, Texas Instruments Inc.). The integrator sampling capacitor was 230 nF and the load resistor was 10 MΩ. The integrator circuit transforms accumulated charge into a voltage signal, which was measured with an oscilloscope (InfiniiVision DSO-X 3024A, Agilent Technologies Inc.). From the peak-to-peak voltage V, the respective charge Q stored in the integrating capacitor C was calculated as

$$Q = C \times V \quad (2)$$

Conclusions

Different ionic liquids were polymerized into electrets with various concentrations from 1 to 20 wt%. Energy generation was evaluated with a custom measurement setup incorporating a charge-integrating amplifier, resulting in charges and charge densities up to 50 nC and 64 nC × cm^{-2}, respectively. Moreover, the energy generated by these electrets was in the range of 0.3–5.5 nJ, providing a power output of up to tens of nanowatts at typical energy harvesting frequencies. The performance can be optimized further by experimenting with the ionic gels, increasing the separation field, and increasing the surface area by micropatterning the electret surface[39] and/or using soft electrodes. To conclude, we demonstrated the performance of ionic liquid electrets as energy harvesters, alongside a robust testing platform and methodology for assessing the novel combinations of ionic liquids and polymers in further pursuits to reach sufficient charge generation for various autonomous devices.

Data availablity

The dataset of the article will be available on Zenodo with following DOI: **10.5281/zenodo.10390799**.

Conflicts of interest

There are no conflicts to declare.

Acknowledgements

The work was funded by the Academy of Finland (project 325185, Nigella) and was also performed as a part of activities of the Johan Gadolin Process Chemistry Centre at Åbo Akademi University in Finland and Chemical-Biological Centre, Umeå University, Sweden. T. Järvinen acknowledges Tauno Tönning and Walter Ahlström foundations for their financial support. The personnel of the Centre for Material Analysis (Univ. Oulu) for the technical assistance and the Swedish Bio4Energy programme are gratefully acknowledged. Topias Järvinen thanks Tauno Tönning and Walter Ahlström foundations for financial support.

References

1 F. U. Khan and M. U. Qadir, *J. Manuf. Syst.*, 2016, **26**, 103001.
2 C. Xu, Y. Song, M. Han and H. Zhang, *Microsyst. Nanoeng.*, 2021, **7**, 1–14.
3 J. Wan, H. Wang, L. Miao, X. Chen, Y. Song, H. Guo, C. Xu, Z. Ren and H. Zhang, *Nano Energy*, 2020, **74**, 104878.
4 X. Wu and D.-W. Lee, *Int. J. Energy Res.*, 2019, **43**, 2402–2409.
5 M. Zhou, M. S. H. Al-Furjan, J. Zou and W. Liu, *Renewable Sustainable Energy Rev.*, 2018, **82**, 3582–3609.
6 Y. Tan, Y. Dong and X. Wang, *J. Microelectromech. Syst.*, 2017, **26**, 1–16.
7 M. Safaei, H. A. Sodano and S. R. Anton, *Smart Mater. Struct.*, 2019, **28**, 113001.
8 H. Wang, M. Han, Y. Song and H. Zhang, *Nano Energy*, 2021, **81**, 105627.
9 Y. Song, H. Wang, X. Cheng, G. Li, X. Chen, H. Chen, L. Miao, X. Zhang and H. Zhang, *Nano Energy*, 2019, **55**, 29–36.
10 S. Ono, *Chem. Rec.*, 2023, **23**, e202300045.
11 S. Yamada, H. Mitsuya and H. Fujita, *J. Phys.: Conf. Ser.*, 2014, **557**, 012013.
12 H. Mitsuya, S. Ono, K. Miwa, M. Ataka, H. Toshiyoshi and H. Fujita, *J. Phys.: Conf. Ser.*, 2015, **660**, 012004.
13 S. Yamada, H. Mitsuya, S. Ono, K. Miwa and H. Fujita, *Proceedings of the IEEE International Conference on Micro Electro Mechanical Systems (MEMS), 2015*, 2015-Febru, pp. 118–121.
14 S. Ono and K. Miwa, *Sens. Mater.*, 2022, **34**, 1853.
15 D. Yamane, K. Tamura, K. Nota, R. Iwakawa, C.-Y. Lo, K. Miwa and S. Ono, *Sens. Mater.*, 2022, **34**, 1869.
16 C. Decker, *Prog. Polym. Sci.*, 1996, **21**, 593–650.
17 C. Gerbaldi, J. R. Nair, G. Meligrana, R. Bongiovanni, S. Bodoardo and N. Penazzi, *J. Appl. Electrochem.*, 2009, **39**, 2199–2207.
18 C. Gerbaldi, J. Nair, C. B. Minella, G. Meligrana, G. Mulas, S. Bodoardo, R. Bongiovanni and N. Penazzi, *J. Appl. Electrochem.*, 2008, **38**, 985–992.
19 J. R. Nair, C. Gerbaldi, G. Meligrana, R. Bongiovanni, S. Bodoardo, N. Penazzi, P. Reale and V. Gentili, *J. Power Sources*, 2008, **178**, 751–757.
20 M. K. Song, J. Y. Cho, B. W. Cho and H. W. Rhee, *J. Power Sources*, 2002, **110**, 209–215.

21 J. G. Huddleston, A. E. Visser, W. M. Reichert, H. D. Willauer, G. A. Broker and R. D. Rogers, *Green Chem.*, 2001, **3**, 156–164.
22 E. I. Rogers, B. Šljukić, C. Hardacre and R. G. Compton, *J. Chem. Eng. Data*, 2009, **54**, 2049–2053.
23 D. S. Silvester and R. G. Compton, *Z. fur Phys. Chem.*, 2006, **220**, 1247–1274.
24 U. Schröder, J. D. Wadhawan, R. G. Compton, F. Marken, P. A. Z. Suarez, C. S. Consorti, R. F. de Souza and J. Dupont, *New J. Chem.*, 2000, **24**, 1009–1015.
25 M. Hayyan, F. S. Mjalli, M. A. Hashim, I. M. AlNashef and T. X. Mei, *J. Ind. Eng. Chem.*, 2013, **19**, 106–112.
26 M. C. Buzzeo, C. Hardacre and R. G. Compton, *ChemPhysChem*, 2006, **7**, 176–180.
27 J. Zhang and A. M. Bond, *Analyst*, 2005, **130**, 1132–1147.
28 A. B. McEwen, H. L. Ngo, K. LeCompte and J. L. Goldman, *J. Electrochem. Soc.*, 1999, **146**, 1687.
29 Z. Wang, Z. Li, Y. Jin, W. Liu, L. Jiang and Q. Zhang, *New J. Chem.*, 2017, **41**, 5091–5097.
30 K. C. Lethesh, S. N. Shah and M. I. A. Mutalib, *J. Chem. Eng. Data*, 2014, **59**, 1788–1795.
31 G. Ara, A. Rahman, M. A. Halim, M. M. Islam, M. Y. A. Mollah, M. M. Rahman and M. A. B. H. Susan, *Mater. Today: Proc.*, 2020, **29**, 1020–1024.
32 S. F. Ghasemi Gildeh, H. Roohi, M. Mehrdad, K. Rad-Moghadam and K. Ghauri, *J. Mol. Struct.*, 2020, **1202**, 127226.
33 C. Sano, H. Mitsuya, K. Ishibashi, S. Ono, K. Miwa, M. Ataka, G. Hashiguchi, H. Toshiyoshi and H. Fujita, *J. Phys.: Conf. Ser.*, 2016, **773**, 012068.
34 S. Yamada, H. Mitsuya, S. Ono, H. Toshiyoshi and H. Fujita, *IEEJ Trans. Sens. Micromachines*, 2019, **139**, 7–14.
35 C. Sano, H. Mitsuya, S. Ono, K. Miwa, H. Toshiyoshi and H. Fujita, *Sci. Technol. Adv. Mater.*, 2018, **19**, 317–323.
36 L. Wu, J. Song, B. Zhang, B. Zhou, H. Zhou, H. Fan, Y. Yang and B. Han, *Green Chem.*, 2014, **16**, 3935–3941.
37 Y. Liu, G. Mao, H. Zhao, J. Song, H. Han, Z. Li, W. Chu and Z. Sun, *Catal. Lett.*, 2017, **147**, 2764–2771.
38 O. Pitkänen, N. Vucetic, H. Cabaud, E. Bozo, T. Järvinen, J.-P. Mikkola and K. Kordas, *Electrochim. Acta*, 2023, 143659.
39 T. Iida, T. Tsukamoto, K. Miwa, S. Ono and T. Suzuki, *Sens. Mater.*, 2019, **31**, 2527.

